RPL9 acts as an oncogene by shuttling miRNAs through exosomes in human hepatocellular carcinoma cells

ANG LI[1,2*], JIYAN XIE[3*], LIHONG LV[4*], ZHIHUA ZHENG[5], WEIBANG YANG[6], WENFENG ZHUO[7], SIJIA YANG[2], DIANKUI CAI[2], JINXIN DUAN[2], PEIQING LIU[5], JUN MIN[2] and JINXING WEI[2]

[1]Guangdong Provincial Key Laboratory of Malignant Tumor Epigenetics and Gene Regulation and [2]Department of Hepatobiliary Surgery, Sun Yat-sen Memorial Hospital, Sun Yat-sen University, Guangzhou, Guangdong 510120; [3]Department of Gastrointestinal Surgery, Peking University Shenzhen Hospital, Shenzhen, Guangdong 518036; [4]Clinical Trial Institution of Pharmaceuticals and [5]Guangdong Provincial Key Laboratory of New Drug Design and Evaluation, Guangdong Province Engineering Laboratory for Druggability and New Drug Evaluation, School of Pharmaceutical Sciences, Sun Yat-sen University, Guangzhou, Guangdong 510120; [6]Department of Hepatobiliary Surgery, The Second Affiliated Hospital of Guangzhou Medical University, Guangzhou, Guangdong 510260; [7]Department of Hepatobiliary Surgery, Fifth Affiliated Hospital, Sun Yat-sen University, Zhuhai, Guangdong 528406, P.R. China

Abstract. The exosomal pathway is an essential mechanism that regulates the abnormal content of microRNAs (miRNAs) in hepatocellular carcinoma (HCC). The directional transport of miRNAs requires the assistance of RNA-binding proteins (RBPs). The present study found that RBPs participate in the regulation of miRNA content through the exosomal pathway in HCC cells. First, differential protein expression profiles in the serum exosomes of patients with HCC and benign liver disease were detected using mass spectrometry. The results revealed that ribosomal protein L9 (RPL9) was highly expressed in serum exosomes of patients with HCC. In addition, the down-regulation of RPL9 markedly suppressed the proliferation, migration and invasion of HCC cells and reduced the biological activity of HCC-derived exosomes. In addition, using miRNA microarrays, the changes in exosomal miRNA profiles in HCC cells caused by RPL9 knockdown were examined. miR-24-3p and miR-185-5p were most differentially expressed, as verified by reverse transcription-quantitative PCR. Additionally, using RNA immunoprecipitation, it was found that RPL9 was directly bound to the two miRNAs and immunofluorescence assays confirmed that RPL9 was able to carry miRNAs into recipient cells via exosomes. Overexpression of miR-24-3p in cells increased the accumulation of miR-24-3p in exosomes and simultaneously upregulated RPL9. Excessive expression of miR-24-3p in exosomes also increased their bioactivity. Exosome-mediated miRNA regulation and transfer require the involvement of RBPs. RPL9 functions as an oncogene, can directly bind to specific miRNAs and can be co-transported to receptor cells through exosomes, thereby exerting its biological functions. These findings provide a novel approach for modulating miRNA profiles in HCC.

Correspondence to: Professor Jinxing Wei or Professor Jun Min, Department of Hepatobiliary Surgery, Sun Yat-sen Memorial Hospital, Sun Yat-sen University, 107 Yanjiang Road, Guangzhou, Guangdong 510120, P.R. China
E-mail: weijx5@mail.sysu.edu.cn
E-mail: minjun@mail.sysu.edu.cn

*Contributed equally

Introduction

Hepatocellular carcinoma (HCC) is the sixth most frequently diagnosed cancer and the third leading cause of cancer-related mortality worldwide (1,2). Exosomes are cell-derived extracellular vesicles (EVs) with a diameter of 40-100 nm (3,4) that contain a large number of biologically active molecules, such as microRNAs (miRNAs), proteins and messenger RNAs (mRNAs) (5). A study has shown that tumor cell-derived exosomes are involved in several cancer processes (6). In addition, miRNAs within exosomes have become the focus of modern research because of their potential roles in tumor development and progression (7).

miRNAs are unstable biomolecules and most miRNAs need to bind to specific RNA-binding proteins (RBPs) to form miRNA-protein complexes in order to exist stably in cells (8);

the dynamic association of miRNAs with RBPs occurs throughout the entire life cycle of miRNA transcription, synthesis, processing, modification, intracellular translocation, functional exertion and degradation (9,10). Accumulating evidence has indicated that miRNA packaging in exosomes is selective (11). However, the molecular mechanisms regulating the profiles of exosomal miRNAs remain to be elucidated. On one hand, HCC cells selectively excrete some endogenous miRNAs to the outside of cells through exosomes. On the other hand, HCC cell-derived exosomes, as essential carriers, can shuttle miRNAs into recipient cells (HCC cells) and promote the proliferation, migration and invasion of recipient cells (12). Therefore, it was hypothesized that some RBPs, as specific proteins bound to miRNAs, may be involved in regulating the profile of exosomal miRNAs in HCC cells.

Ribosomal proteins (RPs) are the components of ribosomes and are RBPs (13). In addition to stabilizing specific ribosomal (r)RNA structures in ribosomal subunits and promoting the correct folding of rRNA, RPs have functions other than protein biosynthesis, known as extra-ribosomal functions (14,15). RPs have also been associated with the occurrence and development of malignant tumors (16).

Ribosomal protein L9 (RPL9) is a member of the 60S subunit of the L6P family of ribosomal proteins (17). However, until recently, only a few studies have reported the relationship between RPL9 and exosomes. The present study focused on the extra-ribosomal functions of RPL9. RPL9 is a cancer-promoting RBP that binds to specific miRNAs and translocates them into exosomes, thereby affecting the profiles of miRNAs within the exosome. Additionally, these miRNAs can enter recipient cells via exosomes and regulate the biological progression of cells. These results initially elucidated the regulatory mechanisms of RBPs in the targeted transport of miRNAs into exosomes and lay the theoretical foundation for exploring exosomal miRNAs interfering with tumor progression.

Materials and methods

Mass spectrometry analysis. Serum exosomes samples were collected from three HCC patients diagnosed with TNM stage I/II, two HCC patients diagnosed with TNM stage III/IV, and three patients with benign liver disease. The proteins in those exosomes were electrophoresed by SDS-PAGE. The gel was stained with Coomassie Blue. The gel with the sample was cut off, digested and analyzed by LC-MS/MS by Bioclouds.

The peptide samples were separated by nano-liter liquid chromatograph (Shimadzu Corporation; cat. no. LC-20AD) at a flow rate gradient of 300 nl/min. The peptides were then transferred to the ESI-tandem mass spectrometer (TripleTOF 5600 LC-MS/MS system; SCIEX). The ion source (Nanospray III source; SCIEX) used a negative ionization mode. The data were collected at an ion source spray voltage of 2,300 V, a nitrogen pressure of 30 psi, and a spray interface temperature of 150°C. The details of the multiple reaction monitoring transitions evaluated were: i) m/z range of 350-1250 Da; ii) the number of charges is 2-5 charges; and iii) the dynamic exclusion of precursor ion was set as follows: The same precursor ion should not undergo fragmentation more than twice within half of the peak-out time, which is approximately 12 sec.

MicroRNA microarrays. Total RNA was isolated from the exosomes of the control group and the RPL9 gene knockdown group. Subsequently, reverse transcriptase was employed to convert RNA into cDNA. The resulting labeled cDNA was then subjected to hybridization with a pre-designed microarray chip. Following scanning of the chip using a scanner, fluorescence signal intensity on each probe was obtained. Specialized software was utilized for data analysis, quality assessment, and differential expression analysis of the scanning results.

Cell lines and culture. SNU387, SNU182 and Hep3B cells were provided by Stem Cell Bank, Chinese Academy of Sciences. MHCC97H cells were purchased from the BeNa Culture Collection (cat. no. BNCC359345) and Huh-7 cells were obtained from Procell Life Science & Technology Co., Ltd. (cat. no. CL-0120). These two cells passed the short tandem repeat analysis and mycoplasma contamination detection. All HCC cell lines were cultured in Dulbecco's modified Eagle's medium (Gibco; Thermo Fisher Scientific, Inc.) containing 10% fetal bovine serum (FBS; Corning, Inc.) at 37°C with 5% CO_2. The FBS used for exosome isolation was depleted of EVs by ultracentrifugation for 12 h at 120,000 x g at 4°C (Optima L-100XP; Beckman Coulter, Inc.).

In vivo tumorigenesis assay. During the experiments, all animals were cared for humanely according to the standards outlined in the 'Guide for the Care and Use of Laboratory Animals' (18). Animal experimental procedures were approved by the Ethics Committee of Sun Yat-Sen University (Guangzhou, China; approval number 2023001498). A total of 21 male athymic nude mice (BALB/c-nu/nu; 5 weeks old; weight ~30 g) were obtained from the Guangdong Medical Laboratory Animal Center. The mice were maintained at a temperature of 26-28°C and relative humidity was maintained at 40-60% with a 10-h/14-h light/dark cycle. Then $1x10^7$ MHCC97H-Control, MHCC97H-RPL9-short hairpin (sh), Huh7-Control and Huh7-RPL9-sh cells were resuspended in 100 μl of Matrigel Matrix (Xiamen Wintop) and injected subcutaneously into the right axilla of nude mice to establish the xenograft tumors.

The specific criteria (i.e., humane endpoints) used to determine whether animals should be sacrificed were: i) Animals on the verge of death, unable to move, or exhibiting no response to gentle stimulation; ii) difficulty in breathing (typical symptoms being salivation and/or cyanosis); iii) diarrhea or urinary incontinence; iv) weight loss of 20% of the pre-experiment weight; v) inability to eat or drink; vi) animals with obvious anxiety, irritability or tumor weight >10% of the animal's own body weight, or tumor rupture; vii) paralysis, persistent epilepsy or stereotyped behavior; viii) skin injury area of the animal accounting for >30% of the whole body, or infection and suppuration; ix) other situations requiring humane end points determined by veterinarians. The experiment lasted for 28 days. Animal health and behavior was monitored once a day.

Of the 21 mice used in the experiment, 20 were sacrificed and one found dead accidentally, the cause unknown. Animal welfare refers to the process of raising, management and use of experimental animals, to take effective measures to make the experimental animals from unnecessary injury, hunger, thirst, discomfort, panic, torture, disease and pain, to ensure

that the animals can achieve natural behavior, by excellent management and care, to provide a clean and comfortable living environment, to provide adequate, ensure the health of food and water, to avoid or reduce pain and suffering. The method of sacrifice was cervical dislocation under deep anesthesia with pentobarbital sodium (30-90 mg/kg; IP). Mortality was verified when the laboratory animal lost consciousness, accompanied by cessation of heartbeat and breathing.

Western blotting. The HCC cells or exosomes were lysed in Western and IP buffers (Key GEN Bio TECH). BCA protein assay kit (Thermo Fisher Scientific, Inc.) was used to measure the protein concentration. Then, the same protein mass (cellular proteins 20 μg per lane; exosome protein 40 μg per lane) was separated by SDS-PAGE on an 11% gel and transferred to polyvinylidene difluoride membranes (Merck KGaA). The primary and secondary antibodies were diluted with universal antibody diluent (cat. no. GF1600-02; Genefist, Inc.). After blocking with 5% skimmed milk for 60 min at room temperature, the membranes were incubated with primary antibody overnight at 4˚C. Finally, the membranes were incubated with the secondary antibody for 60 min at room temperature to visualize the membrane using an enhanced chemiluminescence system (ImageQuant; Cytiva). Western blots were quantified using ImageJ 2.1.0/1.53c (National Institutes of Health) The antibodies were: Apoptosis related gene 2-interacting protein X (Alix; Cell Signaling Technology, Inc.; cat. no. 92880S), tumor susceptibility gene 101 (TSG101; ABclonal Biotech Co., Ltd.; cat. no. A1692), cluster of differentiation (CD)63 (MilliporeSigma; cat. no. SAB4301607), heat shock protein 90 homolog (HSP90; Santa Cruz Biotechnology; cat. no. SC-13119), β-actin (Cell Signaling Technology, Inc.; cat. no. 4970S), GAPDH (Cell Signaling Technology, Inc.; cat. no. 2118S), β-Tubulin (Cell Signaling Technology, Inc.; cat. no. 2146S), RPL9 (Abcam.; cat. no. ab182556), cystathionine β-synthase (CBS; Proteintech Group, Inc.; cat. no. 14787-1-AP), horse anti-mouse IgG horseradish peroxidase (HRP) conjugated secondary antibody (Cell Signaling Technology, Inc.; cat. no. 7076S) and goat anti-rabbit IgG HRP-conjugated secondary antibody (Cell Signaling Technology, Inc.; cat. no. 7074S).

Cytoplasmic and nuclear protein extraction. The nuclear/cytoplasm protein extraction kit (Fudebio-tech; cat. no. FD0199) was used to extract proteins from the nucleus and cytoplasm, respectively, in accordance with the manufacturer's protocols.

RNA isolation and reverse transcription-quantitative (RT-q) PCR. TRIzol® reagent (Thermo Fisher Scientific, Inc) was used for RNA extraction when cell confluence was 70-80%. Prime Script RT Master Mix (Toyobo Life Science) was used for mRNA reverse transcription. Reverse transcription of miRNA was performed using miRNA first-strand cDNA synthesis (tailing method) kit (Sangon Biotech, China). RT-qPCR was performed using SYBR Premix EX Taq TMII (Toyobo Life Science). RNA extraction, cDNA synthesis and qPCR were performed according to the manufacturer's protocols. PCR cycle conditions: Denaturation (95˚C, 30 sec); annealing (95˚C, 5 sec) and extension (60˚C, 30 sec) for 40 cycles. Quantification method was ΔCt=Ct (target gene)-Ct

(internal reference gene), $\Delta\Delta$Ct=ΔCt (experiment group)-ΔCt (control group) and final results were shown as $2^{-\Delta\Delta Cq}$ (12). These experiments were repeated at least 3 times. The internal references for mRNA and miRNA extracted from cells were GAPDH and U6, respectively. However, miRNAs extracted from exosomes used miR16-5p as an internal reference. The primer sequences for RT-qPCR are given in Table SI.

Immunohistochemistry (IHC). The present study analyzed samples from 38 patients who underwent hepatectomy at Sun Yat-sen Memorial Hospital affiliated with Sun Yat-sen University (Guangzhou, China). The patients, ranging in age from 31-72, consisted of 19 individuals with HCC and a male:female ratio of 14:5. In addition, there were 19 patients with benign liver disease and a male:female ratio of 9:10. From the *in vivo* tumorigenicity assay, 20 xenograft tumor tissue samples were obtained in nude mice (MHCC97H-Control tumors, n=4; MHCC97H-RPL9-sh tumors, n=5; Huh7-Control tumors, n=5; Huh7-RPL9-sh tumors, n=6). The antibody used for immunohistochemical detection was anti-RPL9 (Sino Biological; cat. no. 202771-T44). diluted to 1:200 and incubated overnight at 4˚C. Selected tissue images were randomly selected from five fields using the cell imaging system (EVOS FL Auto; Thermo Fisher Scientific, Inc.) and the integrated optical density (IOD) score was assessed using ImageJ 2.1.0/1.53c (National Institutes of Health, USA).

Enzyme linked immunosorbent assay (ELISA). A total of 56 serum samples were collected from HCC patients (age 24-78; male:female ratio 48:8) and 23 from patients with benign liver disease (BLD) (age 27-72; male:female ratio 9:14) at Sun Yat-sen Memorial Hospital affiliated with Sun Yat-sen University (Guangzhou, China), between 2016 and 2018. First, isolated exosome pellets from 100 μl serum were lysed in 100 μl nondenatured protein solubilization reagent (Invent Biotechnologies Inc.) containing a phosphatase-inhibitor and protease-inhibitor (MilliporeSigma). Then the levels were determined using the Human RPL9 ELISA Kit (cat. no. OM516307; Omnimabs, Inc.) according to the manufacturer's instructions.

Patients and specimens. All the human samples were obtained from patients with the written informed consent. The study protocols were approved by the Ethics Committee of Sun Yat-sen Memorial Hospital, Sun Yat-sen University (Guangzhou, China; approval number 2023001498). All research was conducted in accordance with both the Declarations of Helsinki and Istanbul. Patients with a prior diagnosis of primary HCC had not undergone any cancer treatment prior to surgery.

Establishment of stable and transient cell lines. Based on the GV493 vector (Shanghai GeneChem Co., Ltd.), lentiviruses were constructed with knockdown of RPL9 (NM_000661; RPL9-sh-gcGFP; target sequence: gaTGGTATCTATGTCT CTGAA) and control lentiviruses expressing only gcGFP (RPL9-Control-gcGFP; target sequence: TTCTCCGAACGT GTCACGT). When the cell confluence reached 30%, lentivirus was used to infect MHCC97H and Huh7 cell lines. After transfection for 48 h at 37˚C, puromycin was used to screen

with 2 μg/ml. The screening was completed when all cells showed green fluorescence.

Human cDNAs encoding N-terminal Flag-tagged RPL9 (genomic fragments encompassing the CDS sequence 579 bp) were cloned into a pLVX-AcGFP-N1 lentiviral vector to construct the RPL9 expression vector. The primer sequences for cloning were 5'-CCCTCGAGATGGATTACA AGGATGACGACGATAAGAAGACTATTCTCAGCAATC AG-3' (forward) and 5'-CGGGATCCCGTTCATCAGCCT GCTGAACAGTTCC-3' (reverse). The resultant plasmid was designated as pLVX-Flag-RPL9-AcGFP. The human cDNA encoding miR-24-3p (5'-TGGCTCAGTTCAGCAGGAAC AG-3') and miR-185-5p (5'-TGGAGAGAAAGGCAGTTC CTGA-3') were cloned into the pCMV-mChery-SV40-neo vector to construct the vectors pCMV-miR-24-3p-mCherry and pCMV-miR-185-5p-mCherry (fluorescence observation only).

Finally, hsa-miR-24-3p-mimics-Cy5 (5'-UGGCUCAGU UCAGCAGGAACAG-3'), hsa-miR-185-5p-mimics-Cy5.5 (5'-UGGAGAGAAAGGCAGUUCCUGA-3') and the negative control group for the two miRNA-mimics (5'-UUUGUACUA CACAAAAGUACUG-3') were designed and constructed by Nanjing KeyGen Biotech Co., Ltd.

The short interfering (si)RNA sequence sense (5'-3') of human Alix was: GCUCCUGAGAUAUUAUGAUCAUU. The siRNA sequence sense (5'-3') of human VPS4A was: CGAGAA GCUGAAGGAUUAUUUTT. The siRNA sequence sense (5'-3') of human TSG101 was: CAGUCUUCUCUCGUCCUA UUUTT. The control group used for the three siRNAs sequence sense (5'-3') was: UUCUCCGAACGUGUCACGUdTdT.

The transient transfection was conducted in MHCC97H and Huh7 cell lines. Plasmids (1 μg/ml) were introduced when the cell confluence reached 60-80%; miRNA mimics or siRNA (10-50 nmol/l) were added when the cell confluence reached 50%. The transfection process was carried out at 37°C for 24 h using jetPRIME transfection reagent (Polyplus-transfection SA). Laser confocal microscopy or RNA extraction was typically performed after 48 h of transfection, while protein extraction was conducted after 72 h of transfection.

Exosome isolation. The HCC cells were seeded in a 10 cm dish and cultured at 37°C for 2-3 days in a vesicle-depleted medium. The collected media was centrifuged at 300 x g for 10 min, 2,000 x g for 20 min and 10,000 x g for 30 min at 4°C. The supernatant was filtered through a 0.22 μm filter (Millex-GP; MilliporeSigma) to remove large vesicles. The resulting supernatant was further ultracentrifuged at 100,000 x g for 2 h. Alternatively, an appropriate amount of ExoQuick-TC Tissue Culture Media Exosome Precipitation Solution (System Biosciences) was added to isolate exosomes according to the manufacturer's protocols. The exosomes extracted by ultracentrifugation were used for transmission electron microscopy (TEM; JEM-1,400; JEOL, Ltd.) and the reagent-extracted exosomes used for a nanoparticle tracking analyzer (Particle Metrix GmbH), western blotting, PCR and cell co-production cultivation.

Nanoparticle tracking analyzer. The exosome particles, separated from a 10 ml culture medium, were resuspended in 100 μl of PBS. Subsequently, a 10 μl aliquot was taken and diluted to 30 μl with PBS. Operate according to the instructions of the particle size analyzer (N30E; NanoFCM Co., Ltd.). The performance of the instrument was tested with standard substances before the exosome samples were loaded. Note that gradient dilution was required to avoid the blockage of the needle. Following detection, the information regarding the particle size and concentration of exosomes detected by the instrument could be obtained.

TEM. Isolated exosome pellets from 10 ml culture medium were resuspended in 10 μl PBS and fixed with 10 μl paraformaldehyde (4%), absorbed onto the formvar-carbon-coated copper grids for 10 min and dried by filter paper; pellets were then stained with 10 μl uranyl acetate (2%) for 90 sec and dried before examination using TEM operated at 120 kV.

Co-localization experiments with miRNA-mimics transfection. First, RPL9-GFP plasmids, miR-24-3p-mimics-cy5 and miR-185-5p-mimics-cy5.5 were cotransfected with MHCC97H and Huh7 cells, respectively at 37°C for 24 h using jetPRIME transfection reagent (Polyplus-transfection SA). The cells were labeled with PKH26 (PKH26 Red Fluorescent Cell Linker Kit; Beijing Fluorescence Biotechnology Co., Ltd.), which has a fluorescence region of 551-567 nm. According to the manufacturer's protocols, the cells were placed in PKH26 solution and rinsed with serum and complete culture medium after incubation at 25°C for 2-5 min. These cells were cultured in confocal special dishes for 24 h and finally directly observed with a confocal fluorescence microscope (Olympus LV3000; Olympus Corporation).

Confocal laser scanning microscopy. Following transfection of RPL9-GFP and miRNA-mCherry plasmids at 37°C for 24-48 h, the cells were transferred to a glass culture dish and grown for 12 h. The cells were fixed with 4% paraformaldehyde for 15 min at room temperature, treated with 0.3% Triton X-100 for 15 min, stained with DAPI for 10 min and directly observed with a laser confocal microscope (Olympus LV3000, Olympus Corporation).

Exosome and cell co-culture experiments. First, 2x10^7 cells were treated with PKH26, seeded in several 10 cm diameter dishes and cultured at 37°C for 12 h with a vesicle-free medium. When the cell confluence reached 60%, flag-RPL9-AcGFP (1 μg/ml), miR-24-3p-mimics-Cy5 (50 nmol/l) and miR-185-5p-mimics-Cy5.5 (50 nmol/l) were transfected into cells using jetPRIME transfection reagent (Polyplus-transfection SA) and cultured at 37°C for 48 h. Finally, 10 μg of the isolated exosomes was added to a glass culture dish to co-culture with the cells for 12 h and observed under a laser confocal microscope (Olympus LV3000; Olympus Corporation).

RNA immunoprecipitation (RIP). RIP assays were performed using the Magna RIP RNA-Binding Protein Immunoprecipitation kit (MilliporeSigma; cat. no. 17-700) according to the manufacturer's protocols. i) Lysate preparation: serum exosomes isolated from 500 μl of patient serum were utilized as the quantity of exosome lysate for each IP reaction. For MHCC97H and Huh7 cell lines, a total of 2x10^7 cells were employed as the amount of lysate per IP reaction. ii)

Preparation of magnetic beads for immunoprecipitation: 50 μl of magnetic beads protein A/G suspension (the magnetic beads were coated with Protein A or G; MilliporeSigma; cat. no. CS203178) was mixed with RPL9 antibodies (5 μg per IP; Sino Biological; cat. no. 202771-T44) or negative control IgG (5 μg per IP; MilliporeSigma) and incubated for 30 min at room temperature. iii) Immunoprecipitation of RNA-binding Protein-RNA complexes: the lysate obtained from step 1 was mixed with the magnetic beads-antibody complex prepared in step 2 and subjected to overnight incubation at a temperature of 4˚C. Next, the immunoprecipitated RNA was extracted, separated and purified. The total RNA under co-immunoprecipitation of RPL9 protein and IgG in the experiment were transformed into cDNA by using the miRNA first-strand cDNA synthesis (tailing method) kit (Sangon Biotech Co., Ltd.). Finally, the enrichment of binding miRNAs was identified by RT-qPCR.

Co-immunoprecipitation assay (Co-IP). Cells were lysed with IP lysis buffer (Beyotime Institute of Biotechnology) containing protease inhibitors and phosphatase inhibitors (MilliporeSigma). The protein sample (30 μg) was used as input group and the remaining samples were 0.5 mg of cell lysate diluted to 300 μl 1X PBS. Then, 4 μg of anti-RPL9 (Sino Biological; cat. no. 202771-T44) and IgG (cat. no. PP64B; MilliporeSigma) were added respectively, incubated at 4˚C overnight. Then, 50 μl protein A/G magnetic beads (MedChem Express; cat. no. HY-K0202) were added and incubated at room temperature for 4 h. The magnetic beads were washed with 1XPBS with 0.5% Triton, separated by magnetic separation magnetic frame. Subsequently, they were treated with 2X loading buffer (20 μl) and subjected to heat at 95˚C for 5 min in a metal bath. The magnetic beads were isolated by magnetic separation. The interaction between RPL9 protein and other proteins was detected by western blotting.

In order to avoid the influence of IgG heavy chain, rabbit anti-RPL9 and IgG, mouse anti-TSG101 (MilliporeSigma; cat. no. SAB2702167) and VPS4A (Santa Cruz Biotechnology, Inc.; cat. no. SC-393428) and anti-heavy chain secondary antibody (Abbkine Scientific Co.,Ltd.; Anti-Mouse; cat. no. A25012; Anti-Rabbit; cat. no. A25022;) were used. Other antibodies were: Alix (Cell Signaling Technology, Inc.; cat. no. 92880S), CD63 (MilliporeSigma; cat. no. SAB4301607), HSP90 (Santa Cruz Biotechnology; cat. no. SC-13119),

Immunofluorescence (IF). Cells were grown on glass dishes for 24 h then fixed for 15 min in 4% paraformaldehyde and permeabilized with 0.3% Triton X-100 for 15 min at room temperature. Next, cells were blocked with 10% goat serum for 1 h at room temperature, followed by overnight incubation with primary antibodies at 4˚C. After being washed with PBS, the cells were incubated with Alexa-conjugated secondary antibody (Cell Signaling Technology, Inc.) at 37˚C for 1 h and then incubated with DAPI at 37˚C for 5 min. The cells were visualized and images captured on a confocal microscope (Olympus LV3000; Olympus Corporation). Primary antibodies were: RPL9 (dilution: 1:50; Abcam; cat. no. ab182556), TSG101 (dilution: 3:100; MilliporeSigma; cat. no. SAB2702167), VPS4A (dilution: 1:50; Santa Cruz Biotechnology; cat. no. SC-393428) and Alix (dilution: 1:50; Santa Cruz Biotechnology; cat. no. sc-53540).

In vitro cell proliferation, colony formation, migration and invasion assay. The exosomes were diluted to a protein concentration of 10 μg/ml for co-culture with cells.

Cell Counting Kit-8 (CCK-8). Cells (1×10^3) were seeded in 96-well plates. On days 1, 3, 5 and 7 (cells cocultured with exosomes at 12, 24, 48 and 72 h), the cells were treated using Cell Counting Kit-8 (MilliporeSigma) according to the manufacturer's instructions. The OD values of each well were then measured at a wavelength of 450 nm using a multifunctional enzyme marker (Thermo Fisher Scientific, Inc.).

Wound healing assay. Cells were cultured on 6-well plates and scratched with a 10-μl pipette tip when the confluence reached >90%. They were washed three times with PBS and serum-free medium was added and incubate at 37˚C for 3 days. The images were captured under the microscope at 0, 24 and 48 h. Selected images were randomly selected from five fields using the cell imaging system (EVOS FL Auto; Thermo Fisher Scientific, Inc.) at magnification x10.

Transwell migration and invasion assays. The lower chamber was supplemented with 400 μl of DMEM complete medium (Gibco; Thermo Fisher Scientific, Inc.) containing 10% FBS (Corning, Inc.), followed by loading the 8 μm pore size Transwell chambers (Corning, Inc.) and seeding 1×10^5 cells in the upper chamber. For migration assays, the upper chamber was filled with 200 μl of FBS-free DMEM medium. In invasion experiments, a mixture of Matrigel Matrix (Xiamen Wintop) and FBS-free medium (200 μl) was added to the upper chamber. Subsequently, the cells were incubated at 37˚C for 24 h in a cell incubator. Then, cells remaining on the upper surface of the membrane were removed and cells in the lower surface that had passed through the 8 μm hole were fixed with 4% paraformaldehyde and stained with 0.1% crystal violet at 37˚C for 15 min. Finally, those cells were washed and dried with PBS and observed with a transmission light microscope (EVOS FL Auto; Thermo Fisher Scientific, Inc.).

Statistical analysis. The RPL9 expression levels in the HCC and the benign liver disease (BLD) were compared using a paired sample t-test. The relationships between RPL9 expression with the relevant patient and tumor characteristics were analyzed using the χ^2 test. The continuous overall survival (OS) time started from the date of tumor resection until the patient succumbed or was lost to follow-up. Univariate Cox regression analysis was used to understand the relationship between OS and influence factors. Significant prognostic factors were further evaluated by multivariate Cox regression analysis. The Kaplan-Meier curve was used to analyze the effect of a single factor on OS. The statistical analyses were completed by SPSS v23 (IBM Corp.), ImageJ v2.1.0/1.53c (National Institutes of Health) and GraphPad Prism 7.04 (Dotmatics). $P<0.05$ was considered to indicate a statistically significant difference.

Results

RPL9 is upregulated in serum exosomes and clinical samples of patients with HCC. Serum samples were collected from five patients with HCC (C1-C5) and three patients with BLD
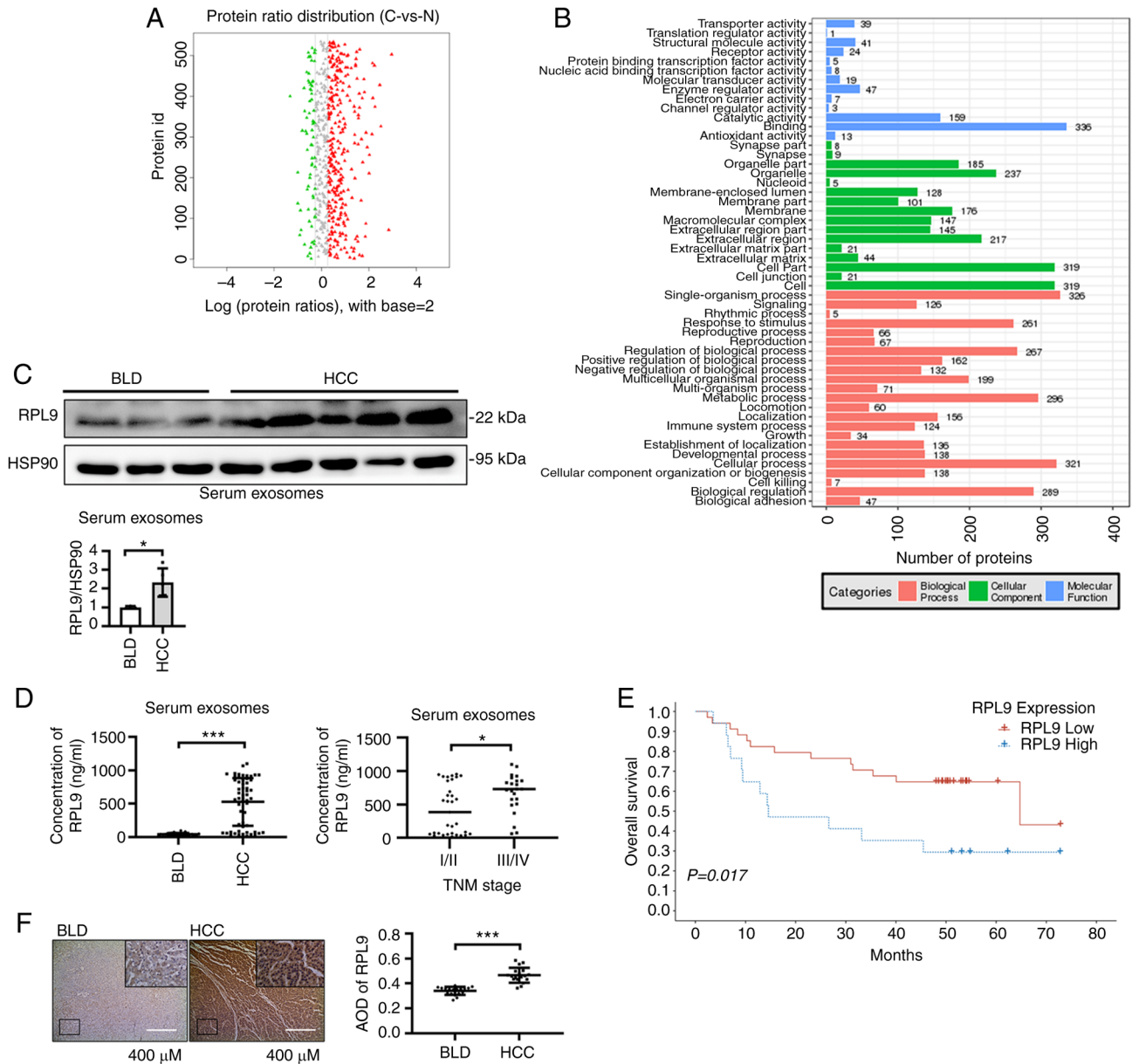
Figure 1. RPL9 is upregulated in serum exosomes and clinical samples of patients with HCC. (A) Analysis of differentially proteins in serum exosomes from patients with BLD (n=3) and HCC (n=5). (B) The detected proteins were classified and functionally analyzed. (C) Western blotting revealed the content of RPL9 in serum exosomes of HCC patients (n=5) was higher than that of BLD (n=3; *P<0.05). (D) ELISA results demonstrated a greater amount of RPL9 in serum exosomes of patients with HCC (n=56) than in patients with BLD (n=23; ***P<0.001). The RPL9 in TNM stage III/IV patients (n=23) were higher than in TNM stage I/II patients (n=33; *P<0.05). (E) The Kaplan-Meier curve showed that a higher level of RPL9 in serum exosomes was associated with shorter overall survival after surgery (P=0.017). (F) Immunohistochemistry results indicated that the content of RPL9 in HCC tissues (n=19) was higher than that in BLD tissues (n=19) (five fields were selected for each tissue, ***P<0.001; scale bar=400 μm). RPL9, ribosomal protein L9; HCC, hepatocellular carcinoma; BLD, benign liver disease; C, Cancer (serum exosomes of HCC); N, Normal (serum exosomes in BLD); AOD, average optical density.

(N1-N3). Exosomes were extracted and subjected to protein profiling. First, the samples were divided into group C (C1-C5) and group N (N1-N3) and the differentially contained proteins in exosomes of HCC patients and BLD patients were obtained after statistical analysis (Fig. 1A; Table SII). Then, proteins with 'RNA-binding' function were screened out from the 'binding' classification of cluster analysis (Fig. 1B; Table SIII). Finally, seven RBPs (RPL9, RPL28, RPS13, RPS14, RPS4X, PSMA6 and SNU13) were found to be highly contained in serum exosomes of HCC patients. Since C1-C2 was derived from HCC patients with TNM stage I/II and C3-C5 was derived from HCC patients with TNM stage III/IV, the samples were

again divided into CA (C1-C2), CB (C3-C5) and N (N1-N3) groups. By analyzing the content of RNA binding protein in the three groups (Fig. S1A; Tables SIV, SV and SVI), the present study screened RPL9 genes, which was not only highly contained in the serum exosomes of HCC patients, but also had a higher content in the serum exosomes of TNM stage III/IV HCC patients (Fig. S1B).

Western blotting experiments initially verified the content of RPL9 in serum exosomes of five HCC patients and three BLD patients (Fig. 1C). To further verify the difference in RPL9 content, the sample collection was expanded. ELISA showed that the content of RPL9 in the serum exosomes of

patients with HCC (56 cases) was significantly higher than that in the serum exosomes of patients with BLD (23 cases). In patients with HCC, the serum exosome RPL9 was generally higher in TNM stage III/IV (23 cases) compared with TNM stage I/II (33 cases; Fig. 1D). Data on 56 patients with HCC was then gathered and followed up, finally obtaining prognostic information on 51 patients with HCC after excluding patients who had missed follow-up. Based on the optimal cut-off value, patients with HCC were divided into high-risk (RPL9 high) and low-risk (RPL9 low) groups (their clinico-pathological characteristics are presented in Table SVII). The analysis revealed that higher serum exosome RPL9 levels were a risk factor for postoperative survival (Fig. 1E; Tables SVIII and SIX). In addition, 19 HCC and 19 BLD tissue samples were selected and their IHC analyses showed that RPL9 was more highly expressed in HCC tissues than in BLD tissues (Fig. 1F). By examining clinical samples, it was determined that the RBP RPL9 was upregulated in serum exosomes and cancer tissues, suggesting that this gene may be associated with cancer-promoting effects in humans.

Downregulation of RPL9 suppresses the ability of HCC cells to proliferate, migrate and invade. To evaluate the role of RPL9 in HCC more fully, the expression of RPL9 in different hepatoma cell lines (SNU387, SNU182, Hep3B, Huh7 and MHCC97H) and their secreted exosomes was examined (Fig. 2A). As the RPL9 protein was strongly expressed, lentiviruses were designed with the knocked-down RPL9 gene and control viruses. MHCC97H and Huh7 were then selected to construct stably transfected cell lines and the cells divided into control (MHCC97H-control and HuH7-control) and RPL9-sh groups (MHCC97H-RPL9-sh and HuH7-RPL9-sh) for comparison (Fig. 2B).

Next, CCK-8 (Fig. 2C), clone formation (Fig. 2D), wound healing (Fig. 2E) and Transwell assays (Fig. 2F) were performed and it was found that the proliferation, migration and invasion abilities of MHCC97H and Huh7 cells were significantly inhibited when RPL9 was knocked down. These results indicated that downregulation of RPL9 suppressed the progression of HCC, suggesting that RPL9 may function as an oncogene.

Downregulation of RPL9 affects the profile of miRNAs in the exosomes of HCC cells. EVs were extracted from the culture medium supernatant of the HCC cells. Nanoparticle tracking analysis showed that most of the EVs were in the range of 40-100 nm (Fig. 3A). TEM revealed a smooth, cup-shaped envelope (Fig. 3B). Meanwhile, western blotting showed that EVs contained typical exosome markers (Alix, HSP90, TSG101 and CD63; Fig. 3C). These results suggest that the isolated EVs have typical characteristics of exosomes. It was also found that downregulation of RPL9 significantly reduced RPL9 protein content at the exosome level (Fig. 3D).

As an RBP, RPL9 is widely involved in the biosynthesis, transport and binding of miRNAs and is abundant in exosomes. The present study examined the effect of RPL9 on the miRNA profile in HCC exosomes and screened miRNAs that were significantly altered with the reduction of RPL9 protein in exosomes using miRNA microarray technology (Fig. 3E; Tables SX and SXI).

Downregulation of RPL9 results in differential expression of miR-24-3p and miR-185-5p and affects the biological activity of exosomes derived from HCC cells. To further verify the reliability of the selected miRNAs, the profile changes of some miRNAs after RPL9 knockdown were examined (Fig. S2). However, it was found that the content of these miRNAs was not consistent between cells and exosomes. Most of the miRNAs were increased or unchanged in the cells, but were clearly reduced in the exosomes. In particular, miR-24-3p and miR-185-5p showed significantly decrease in cells and exosomes (Fig. 4A). It was hypothesized that the downregulation of RPL9 would inhibit the transfer of several miRNAs into exosomes and that there could be interactions between RPL9 and miR-24-3p or miR-185-5p.

Our previous experiments revealed that HCC cell-derived exosomes promote the biological behavior of parent HCC cells (12). As RPL9 can affect the profile of exosomal miRNAs, it was hypothesized whether RPL9 affects the biological activity of exosomes. After the exosomes secreted by the cells in the RPL9-control group and the RPL9-sh group were extracted, the exosomes were diluted to a protein concentration of 10 μg/ml and co-incubated with the recipient cells, changing the fluid every 24 h. Using CCK-8, wound healing and Transwell assays (Fig. 4B-D), it was found that knockdown of RPL9 inhibited the proliferation, migration and invasion abilities of the recipient cells. This suggested that RPL9 downregulation markedly suppressed the biological activity of HCC cell-derived exosomes.

Overexpression of RPL9 facilitates miR-24-3p and miR-185-5p entry into the recipient cells via the exosome pathway. It was hypothesized that RPL9 may be closely related to miR-24-3p and miR-185-5p. To further explore this relationship, the present study first transfected the pLVX-Flag-RPL9-AcGFP plasmid into MHCC97H and Huh7 cells to construct an RPL9 overexpression cell line. The RPL9 control cell line was constructed by transfecting cells with the empty plasmid pLVX-Flag-AcGFP. After verifying the expression of RPL9 (Fig. 5A), it was found that the content of miR-24-3p and miR-185-5p were elevated in both cells and exosomes when RPL9 protein expression was enhanced (Fig. 5B). Based on the consistency between RPL9 and miRNA changes, it was hypothesized that RPL9 may promote the biological properties of tumors in an miRNA-dependent manner.

While it was hypothesized that changes in miRNA profiles in exosomes affected the biological progression of recipient cells, it was unclear whether RPL9 and miRNAs can enter cells via exosomes. To test this, cells were stained with the membrane structural marker PKH26 (red) and then successively transfected them with the fusion plasmids pLVX-Flag-RPL9-AcGFP (green), miR-24-3p-mimics-cy5 (orange) and miR-185-5p-mimics-cy5.5 (purple); the collected exosomes were co-cultured with the original cells. The fluorescence was visualized inside the recipient cells using laser confocal microscopy (Fig. 5C), suggesting that RPL9, miR-24-3p and miR-185-5p were present in the exosomes and were then transferred to fresh cells with exosomes. These data indicated that RPL9 may bind to and carry miRNAs that play a role through exosomes.
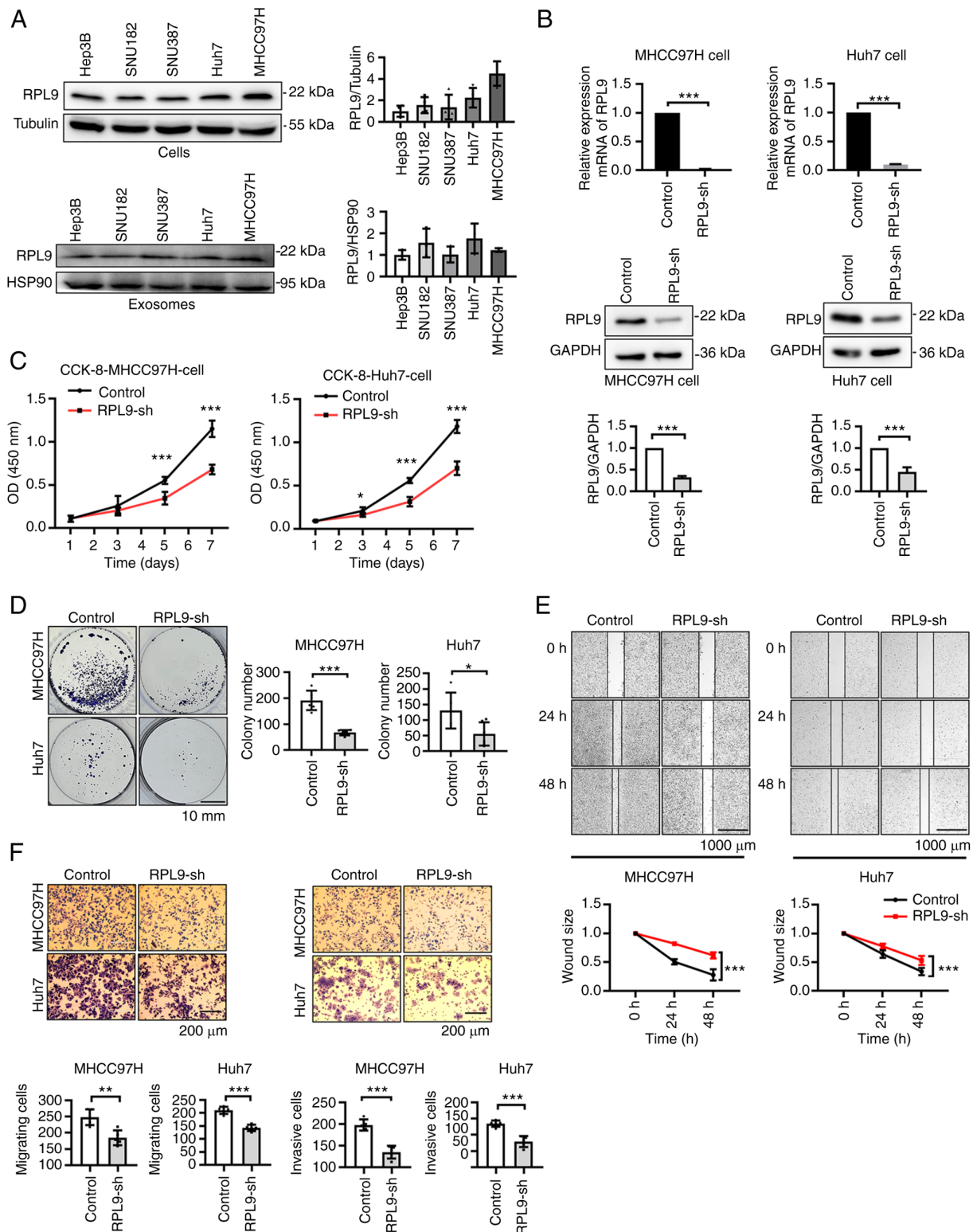
Figure 2. Downregulation of RPL9 suppresses the ability of HCC cells to proliferate, migrate and invade. (A) Western blotting to detect the expression of RPL9 in five human HCC cell lines (Hep3B, SNU182, SNU387, Huh7, MHCC97H) and their secreted exosomes. (B) Stably expressed RPL9 knockdown (RPL9-sh) and control cell lines were constructed in MHCC97H and Huh7 cells. Western blotting and reverse transcription-quantitative PCR experiments were used to verify the expression level of RPL9 (***P<0.001). (C) CCK-8 (n=5; ***P<0.001) and (D) cell colony formation assays (n=6; *P<0.05, ***P<0.001; scale bar=10 mm) indicated that RPL9 downregulation hindered cell proliferation. (E) Wound healing (n=6; ***P<0.001; scale bar=1,000 μm) revealed that RPL9 silence reduced cell migration capacity. (F) Transwell migration and Transwell invasion experiment (n=5; **P<0.01, ***P<0.001; scale bar=200 μm) suggested that the migration and invasion abilities were suppressed after RPL9 knockdown. RPL9, ribosomal protein L9; HCC, hepatocellular carcinoma; sh, short hairpin.

RPL9 directly binds to miR-24-3p and miR-185-5p. To verify whether RPL9 protein and miRNA bind to each other in cells and exosomes, an RIP assay was performed using serum

exosomes from patients with HCC, MHCC97H cells and Huh7 cells as lysates. Subsequently, miRNAs screened by the miRNA microarray were selected for validation (Fig. S3A-C)
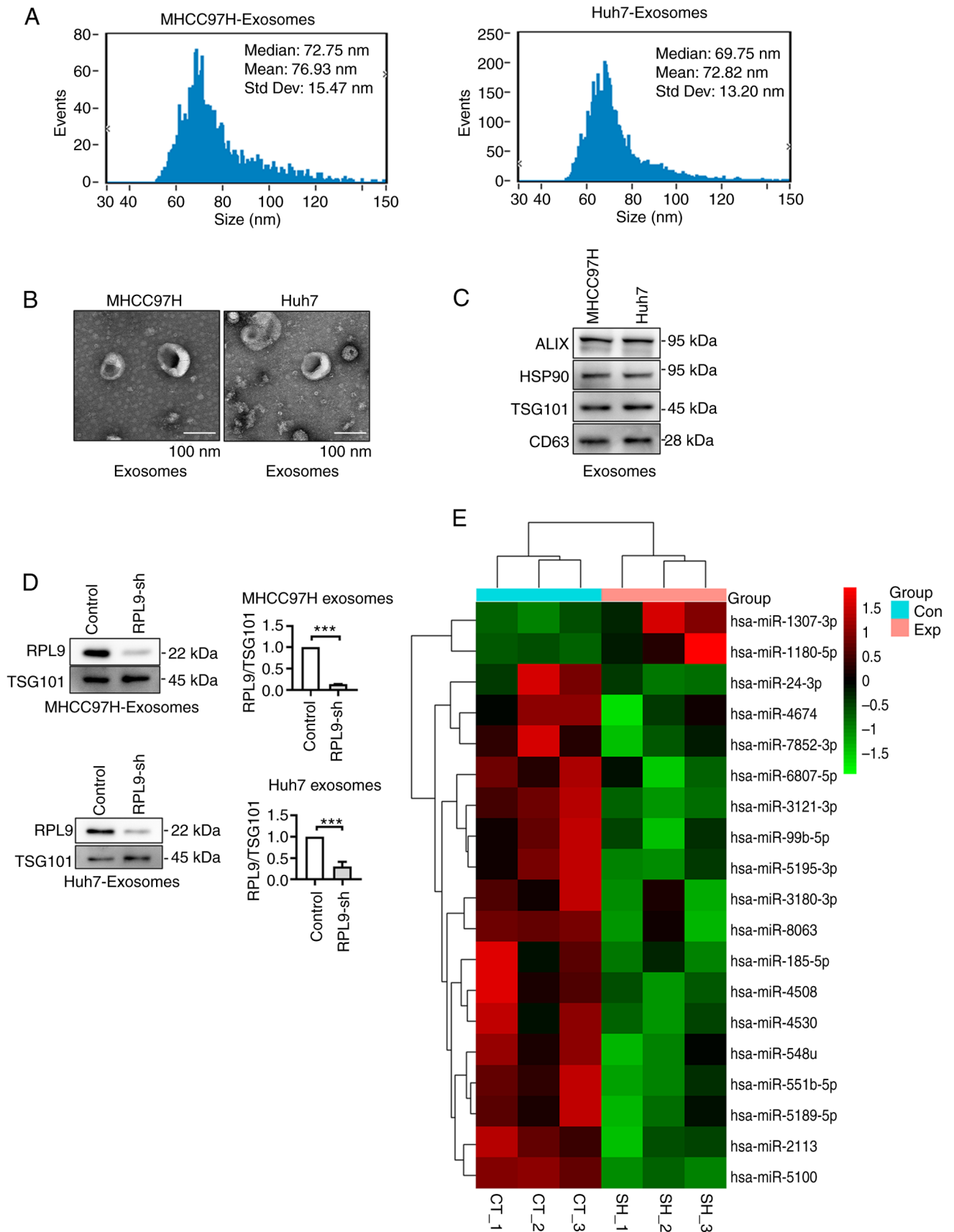
Figure 3. Downregulation of RPL9 affects the profile of miRNAs in the exosomes of HCC cells. (A) NTA results indicated that the size of the isolated exosomes was mainly distributed at 40-100 nm. (B) Transmission electron microscopy showed the classic cup-like structure of exosomes secreted by MHCC97H and Huh7 cells (scale bar=100 nm). (C) The isolated exosomes contained representative exosome markers (Alix, HSP90, TSG101 and CD63) in western blotting. (D) Western blotting showed that downregulation of RPL9 in the cells resulted in decreased secretion of RPL9 in exosomes (***P<0.001). (E) Heat map revealed the differentially content miRNAs into exosomes released from control cells (CT_1-3) and RPL9 knockdown (SH_1-3) cells (P<0.05). RPL9, ribosomal protein L9; miRNA/miR, microRNA; HCC, hepatocellular carcinoma; sh, short hairpin; Con, control; Exp, expression decrease; CT, MHCC97H control cell-derived exosomes; SH, MHCC97H-RPL9-sh cell-derived exosomes.
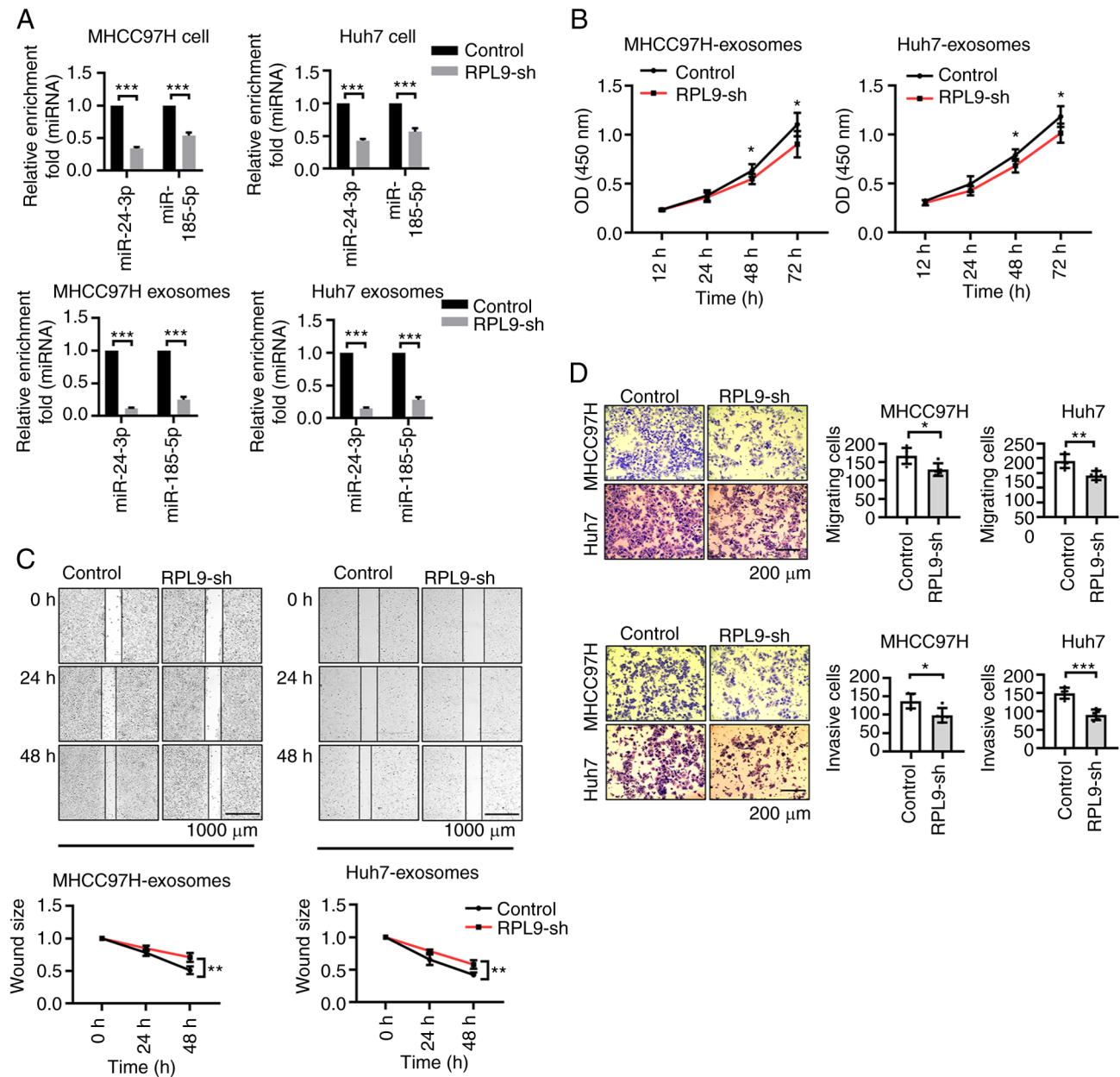
Figure 4. Downregulation of RPL9 results in differential expression of miR-24-3p and miR-185-5p and affects the biological activity of exosomes derived from HCC cells. (A) Reverse transcription-quantitative PCR showed that the content of miR-24-3p and miR-185-5p in cells and exosomes were distinctly decreased with the knockdown of RPL9 (***$P<0.001$). The present study co-cultured exosomes (10 μg/ml, exosomes were diluted to a protein concentration of 10 μg/ml) from the RPL9-control and RPL9-sh groups with recipient HCC cells, respectively. From (B) CCK-8 (n=6; *$P<0.05$), (C) wound healing (n=6; **$P<0.01$; scale bar=1,000 μm) and (D) Transwell assays (n=5; *$P<0.05$, **$P<0.01$, ***$P<0.001$; scale bar=200 μm), recipient cell proliferation, migration, invasion abilities were relatively reduced after receiving exosomes from the RPL9-sh group. RPL9, ribosomal protein L9; miRNA/miR, microRNA; HCC, hepatocellular carcinoma; sh, short hairpin.

and it was found that miR-24-3p and miR-185-5p could directly bind RPL9 in both HCC cells and exosomes (Fig. 6A-C).

To further determine the interactions among RPL9, miR-24-3p and miR-185-5p, fusion plasmids were designed (pLVX-Flag-RPL9-AcGFP, pCMV-miR24-3p-mCherry and pCMV-miR-185-5p-mCherry) and transfected into MHCC97H and Huh7 cells. Co-localization experiments showed that the green light emitted by RPL9 could fuse with the red light emitted by miR-24-3p or miR-185-5p (Fig. 6D). This suggested the possible mutual binding of RPL9 with miR-24-3p or miR-185-5p. It was also observed that plasmid-generated fluorescence tended to aggregate

within the cell; therefore, it was hypothesized that this may be a manifestation of RPL9 and miRNA enrichment in multivesicular bodies. Next, the cells were transfected with pLVX-Flag-RPL9-AcGFP (green), miR-24-3p-mimics-cy5 (orange) and miR-185-5p-mimics-cy5.5 (purple), followed by PKH26 (red) staining of the cell membrane. Using laser confocal microscopy, the present study not only visualized the co-localization phenomenon, but also more precisely observed the enrichment of RPL9, miR-24-3p and miR-185-5p in the intracellular spherical membrane structure (Fig. 6E). These results indicated that RPL9 may bind directly to miR-24-3p and miR-185-5p in both cells and exosomes.
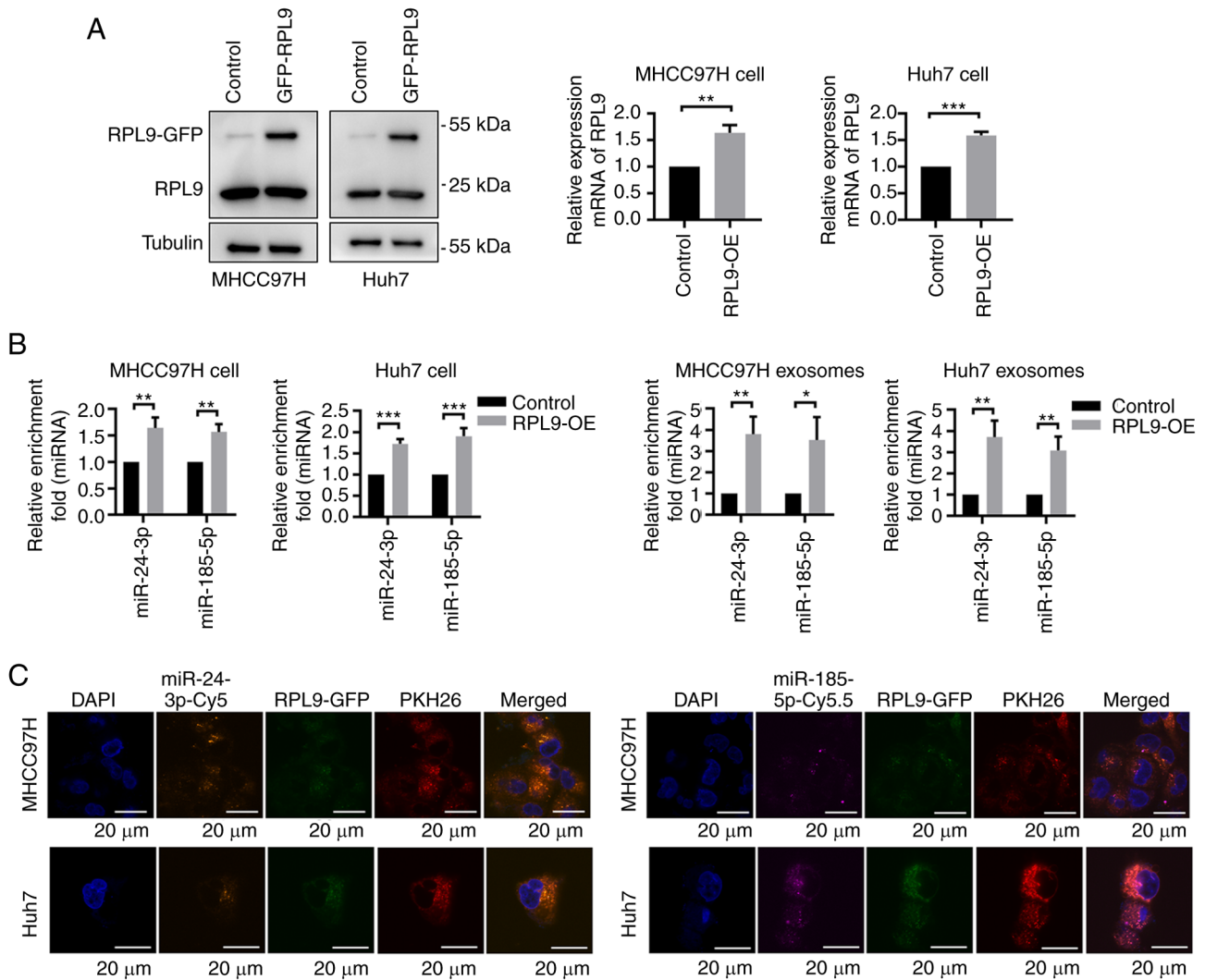
Figure 5. Overexpression of RPL9 facilitates miR-24-3p and miR-185-5p entry into the recipient cells via the exosome pathway. (A) In the RPL9 overexpression cell lines, reverse transcription-quantitative PCR and western blot experiments were performed to verify their expression effect (**P<0.01, ***P<0.001). (B) When RPL9 protein expression was enhanced, miR-24-3p and miR-185-5p were subsequently elevated in cells and exosomes (*P<0.05, **P<0.01, ***P<0.001). (C) The cells were treated with PKH26 (red) and transfected with fusion plasmids Flag-RPL9-AcGFP (green) and miR-24-3p-mimics-Cy5 (orange), miR-185-5p-mimics-Cy5.5 (purple), their exosomes were extracted and co-cultured with fresh original cells. The fluorescence could be observed in the recipient cells (scale bar=20 μm). RPL9, ribosomal protein L9; miRNA/miR, microRNA; RPL9-OE, RPL9-over expressed; GFP, green fluorescent protein; DAPI, 4',6-diamidino-2-phenylindole; Cy, cyanine.

Downregulation of RPL9 suppresses the growth of HCC tumors and reduces miR-24-3p and miR-185-5p content in vivo. To investigate the role of RPL9 *in vivo*, the present study performed subcutaneous graft tumor formation experiments in naked mice. During cancer growth, it was noted that the neoplasm volume (Fig. 7A) and mass (Fig. 7B) of mice injected with RPL9-sh cells were distinctly smaller than those of mice injected with control cells. An IHC assay was used to detect the expression level of RPL9 in tumor tissues (Fig. 7C). RT-qPCR found that miR-24-3p and miR-185-5p in tissues decreased when RPL9 was downregulated (Fig. 7D). Finally, to understand the changes in human-derived miRNAs in mice, exosomes were extracted from the circulating blood of mice for RT-qPCR. The results showed that RPL9 inhibition led to a reduction in the amount of miR-24-3p and miR-185-5p in the exosomes released by cancer cells (Fig. 7E). The *in vivo* study revealed that RPL9 is oncogenic and modulates the profiles of miR-24-3p and miR-185-5p in exosomes.

Overexpression of miR-24-3p promotes the biological activity of exosomes and causes an upregulation of RPL9 in exosomes. It was hypothesized that RPL9 probably plays a role in regulating miRNA transport via the exosomal pathway in HCC cells. When miR-24-3p was overexpressed in RPL9 control HCC cells, the content of miR-24-3p in exosomes secreted by HCC cells was clearly increased. However, overexpression of the same dose of miR-24-3p in RPL9 knockdown cells did not significantly alter the amount of miR-24-3p in exosomes (Fig. 8A). After overexpression of miR-24-3p in RPL9 control cells, RPL9 protein was increased in both cytoplasm and exosomes to varying degrees. Nevertheless, after overexpression of miR-24-3p in RPL9 knockdown cells, the changes of RPL9 protein and miR-24-3p in exosomes tended to be normal (Fig. 8B). It was hypothesized that excessive miR-24-3p could stimulate the transport of RPL9 to exosomes, resulting in the secretion of more RPL9-miR-24-3p complexes into the exosomes; however, when the intracellular level of
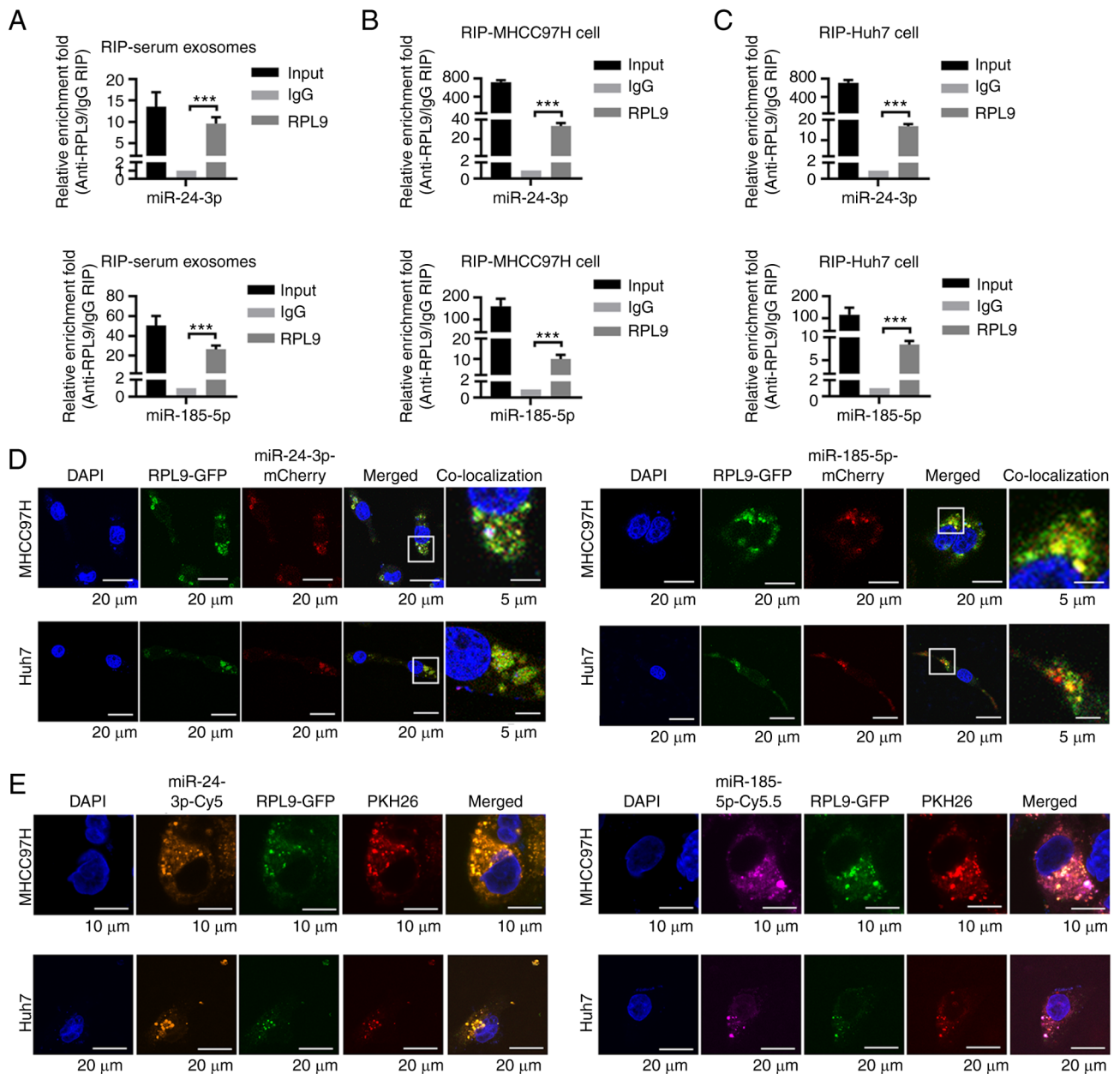
Figure 6. RPL9 directly binds to miR-24-3p and miR-185-5p. RIP assay was performed using (A) serum exosomes from HCC patients, (B) MHCC97H cells and (C) Huh7 cells as lysates. Reverse transcription-quantitative PCR results showed that among these three substrates, miR-24-3p and miR-185-5p could bind directly to RPL9 (***P<0.001). (D) Confocal laser scanning microscopy revealed the colocalization of RPL9-GFP with miR-24-3p-mCherry and miR-185-5p-mCherry (scale bar=20 µm; scale bar=5 µm). (E) Subsequently, cells were transfected with pLVX-Flag-RPL9-AcGFP (green), miR-24-3p-mimics-cy5 (orange) and miR-185-5p-mimics-cy5.5 (purple), followed by staining the cell membrane with PKH26 (red). RPL9, miR-24-3p and miR-185-5p were enriched in the intracellular spherical membrane structure (scale bar=10 µm; scale bar=20 µm). RPL9, ribosomal protein L9; miRNA/miR, microRNA; RIP, RNA immunoprecipitation; HCC, hepatocellular carcinoma.

RPL9 was low, this process might be inhibited. The exosomes secreted by the RPL9 control cells miR-24-3p-control group, the RPL9 control cells miR-24-3p overexpression group and the RPL9 knockdown cells miR-24-3p overexpression group were extracted. After co-culturing exosomes (10 µg/ml) with cells, CCK-8 (Fig. 8C), wound healing (Fig. 8D) and Transwell assays (Fig. 8E) were used and it was found that the increase of miR-24-3p in exosomes promoted the proliferation, migration and invasion of receptor cells compared with that of negative control cells. However, the exosomes secreted by HCC cells after simultaneous downregulation of RPL9 and upregulation of miR-24-3p did not cause phenotypic changes in recipient

cells. Therefore, it was hypothesized that the biological progression of recipient HCC cells after co-culturing with exosomes may be related to difference miRNA content in exosomes.

Overexpression of miR-24-3p results in CBS downregulation in the recipient cell via the exosome pathway. It was hypothesized that exosomal miR-24-3p transported into recipient HCC cells via RPL9 may facilitate their biological progression by directly affecting downstream targets. One study (19) demonstrated that miR-24-3p is a direct upstream regulator of CBS. As a tumor suppressor, CBS exerts anti-liver cancer effects
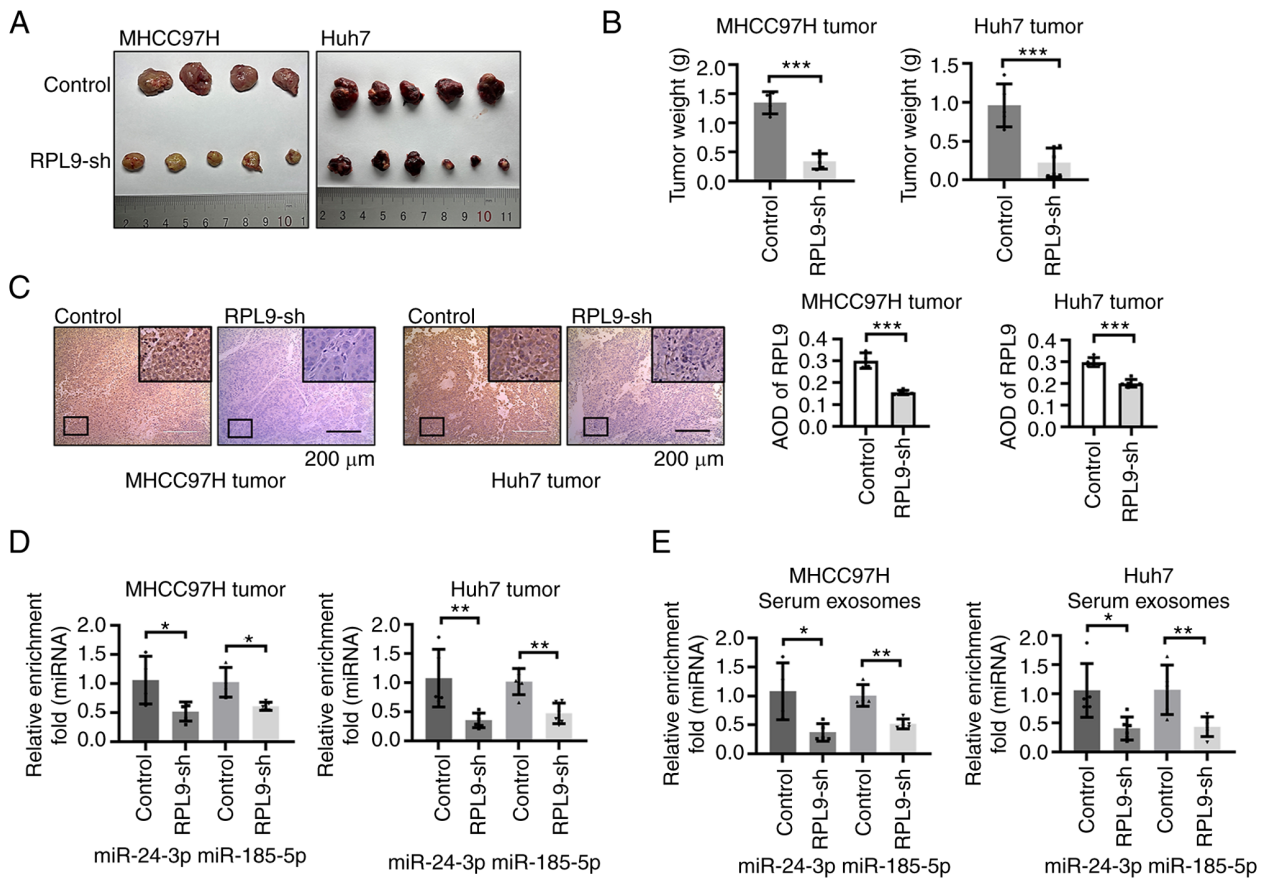
Figure 7. Downregulation of RPL9 suppresses the growth of HCC tumors and reduces miR-24-3p and miR-185-5p content *in vivo*. (A) Images of xenografts. HCC cells were subcutaneously injected into the right axilla of 5-week-old male BALB/c-nu/nu mice. One mouse died accidentally leaving 20 tumor-bearing mice (MHCC97H-Control tumors, n=4; MHCC97H-RPL9-sh tumors, n=5; Huh7-Control tumors, n=5; Huh7-RPL9-sh tumors, n=6). (B) At 28 days after HCC cell implantation, the tumor weight of RPL9-sh group was significantly less than that of the RPL9-control group (***$P<0.001$). (C) Immunohistochemistry demonstrated that the expression level of RPL9 in the RPL9-sh group were clearly lower than control (five fields were selected for each tissue; ***$P<0.001$; scale bar=200 μm). Reverse transcription-quantitative PCR showed that the number of miR-24-3p and miR-185-5p in (D) tumor cells and (E) mouse serum exosomes decreased with RPL9 knockdown (*$P<0.05$, **$P<0.01$). RPL9, ribosomal protein L9; HCC, hepatocellular carcinoma; miRNA/miR, microRNA; sh, short hairpin.

by inhibiting the PRRX2/IL-6/STAT3 pathway. Therefore, the exosomes (10 μg/ml) secreted from cells in the miR-24-3p overexpression and control groups were co-cultured with the recipient cells. The results revealed that CBS gene expression in the target cells was downregulated after receiving more miR-24-3p-containing exosomes (Fig. 8F). This suggested that miRNAs in exosomes can be delivered to another cell and function at the new location.

Discussion

Abnormal miRNA profiles are important in the development and occurrence of liver cancer. Exosomes are essential for HCC cells to regulate the profile of their miRNAs, which can enter and function in recipient cells via exosomes (20,21). By contrast, the mechanism of selective entry of miRNAs into exosomes was previously unknown; however, because of the specificity of the RNA structure, it was hypothesized that there must be a transport mechanism in cells that can load the miRNA cargo into the exosomes and that RNA transport to exosomes probably occurs through the action of certain RBPs. Our previous study (12) showed that the exosome regulatory factor Vps4A, an accessory molecule (22,23) of endosomal sorting complexes required for

transport (ESCRT), affects the secretion of miRNAs in HCC cells and the uptake of miRNAs by recipient cells through exosomes. Altering the integrity of ESCRT usually interferes with the RBP GW182, consequently impairing miRNA function (24). GW182 protects mature miRNAs from degradation by interacting with argonaute and knockdown of GW182 reduces miRNA secretion via exosomes (25). In addition, some RBPs, such as YBX1 and hnRNPA2B1, are capable of directly sorting miRNAs into exosomes (26,27). Therefore, it was hypothesized that RBPs may be involved in regulating the process of miRNA packaging into exosomes in HCC cells and that this process may be one of the mechanisms leading to the anomalous profile of miRNAs in HCC cells.

Thus, mass spectrometry analysis was performed on serum exosome samples from patients with BLD and HCC and several differentially expressed RBPs were screened. Among these, RPL9, RPL28, RPS13, RPS14 and RPS4X are ribosome-binding proteins. Ribosome is a stable and ancient protein-RNA complex (28) and ribosome-binding proteins have both RNA-binding properties and protein-protein interaction domains, providing natural advantages in RNA transport and regulation (29). RPL9, which was highly contained in the serum exosomes of patients with HCC, was selected to
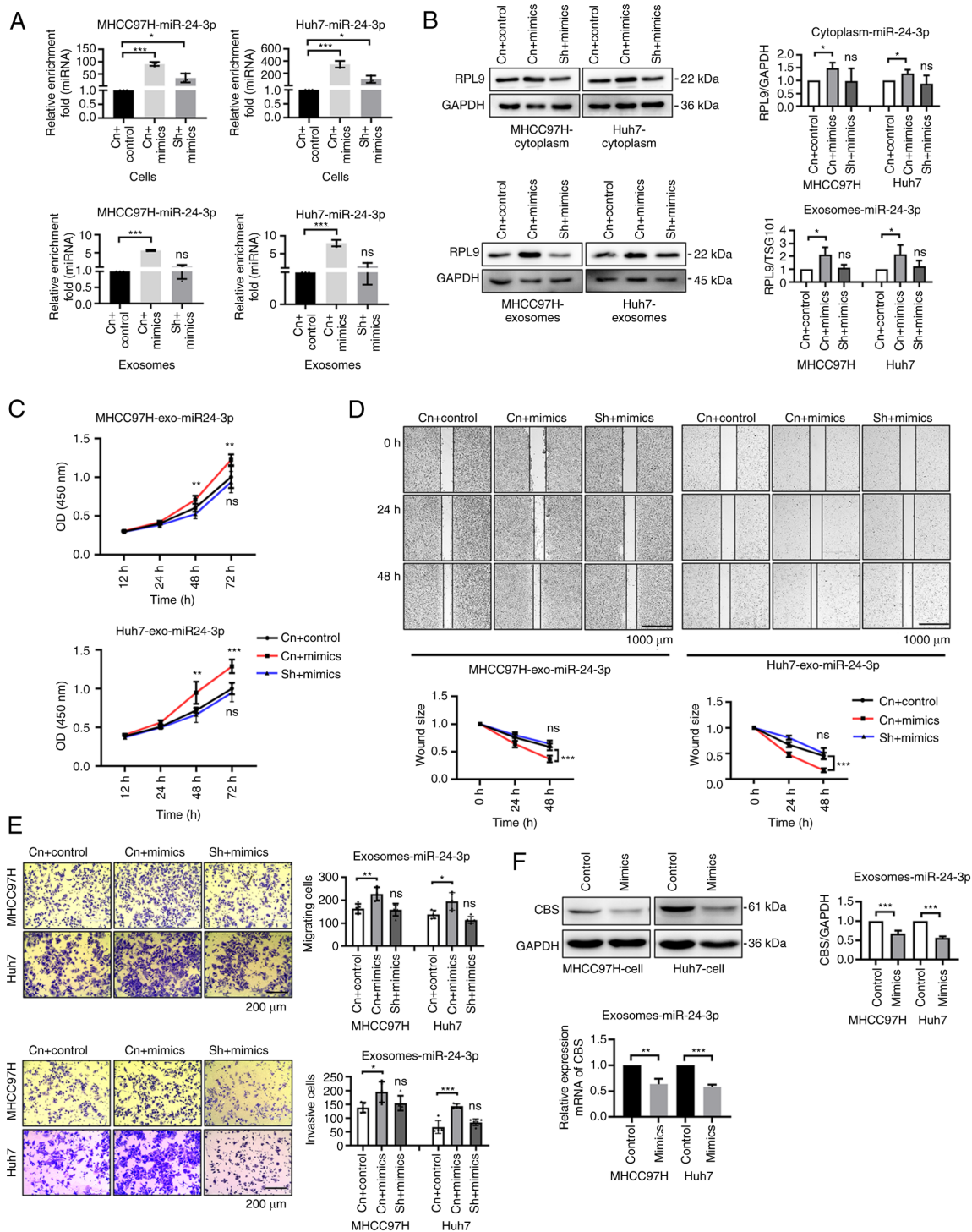
Figure 8. Overexpression of miR-24-3p promotes the biological activity of exosomes and causes an upregulation of RPL9 in exosomes. Following transfection with miR-24-3p-mimics into RPL9 control and RPL9 silenced HCC cells, (A) reverse transcription-quantitative PCR showed that miR-24-3p was significantly increased in cells and exosomes of RPL9 control cells. Meanwhile, the miR-24-3p exhibited a slight increase in cells with RPL9 silenced, while exosomes showed little alteration (nsP>0.05; *P<0.05; ***P<0.001). (B) Western blotting results showed a relative increase in RPL9 protein content in both the cytoplasm and exosomes of cells in the RPL9 control group, while no significant difference was observed between the cytoplasm and exosomes of cells in the RPL9 silencing group (nsP>0.05; *P<0.05). RPL9 control cells were transfected with the miR-24-3p-control and the miR-24-3p mimic, followed by transfection of the miR-24-3p mimic into RPL9 knockdown cells. Finally, recipient HCC cells were co-cultured with extracted exosomes (10 µg/ml). From (C) CCK-8 (n=6; nsP>0.05; **P<0.01, ***P<0.001), (D) wound-healing (n=6; nsP>0.05; ***P<0.001; scale bar=1,000 µm) and (E) Transwell assays (n=5; nsP>0.05; *P<0.05, **P<0.01, ***P<0.001; scale bar=200 µm), it was observed the exosomes, secreted by RPL9 control cells receiving miR-24-3p-mimics, caused a relative enhancement in the proliferation, migration, and invasion of recipient cells. However, the exosomes secreted by RPL9 knockdown cells receiving miR-24-3p-mimics did not caused significant differences in those abilities of recipient cells. Overexpression of miR-24-3p resulted in CBS downregulation in the recipient cell via the exosome pathway. (F) Exosomes secreted by the miR-24-3p-control group and the overexpression group were extracted and co-cultured (10 µg/ml) with the recipient cells. Western blotting and reverse transcription-quantitative qPCR experiments showed that CBS gene expression in target cells was substantially downregulated after receiving more miR-24-3p exosomes (**P<0.01, ***P<0.001). miRNA/miR, microRNA; RPL9, ribosomal protein L9; HCC, hepatocellular carcinoma; CBS, cystathionine β-synthase; Cn + control, the miR-24-3p-control group into RPL9 control cells; Cn + mimics, the miR-24-3p-mimics group into RPL9 control cells; sh + mimics, the miR-24-3p-mimics group into RPL9 knockdown cells; ns, no significance; Control, the miR-24-3p-control group into HCC cells; Mimics, the miR-24-3p-mimics group into HCC cells.

continue the present study. RPL9 is an abundant RBP with various extra-ribosomal functions. For example, defects in ribosome synthesis lead to cell cycle arrest or apoptosis (30); genetic variants of RPL9 promote the development of certain diseases or types of cancer (31); and RPL9 interacts with Gag proteins and affects viral assembly (32). In addition, after long-term follow-up of patients with HCC, the increase of RPL9 protein in serum exosomes was an influencing factor for poor prognosis. Thus, the level of RPL9 in circulating exosomes could be used as a biomarker to predict the prognosis of patients with HCC. By suppressing the expression of RPL9 in HCC cells, their proliferation, migration and invasion abilities were inhibited. Its role in regulating the biological behavior of cancer cells has previously been demonstrated in colon cancer (33). Therefore, it was hypothesized that RPL9 promotes HCC progression and that RPL9 may carry miRNAs into exosomes in the form of RPL9-miRNAs interaction similar to some RBPs. Based on this hypothesis, miRNA microarray technology was used to screen for miRNAs that were significantly altered in the exosomes of MHCC97H cells following RPL9 knockdown. The results showed that RPL9 affects the profile of exosomal miRNAs and most of these altered miRNAs have oncogenic effects on HCC cells. Next, the present study confirmed by RIP and co-localization experiments that RPL9, miR-24-3p and miR-185-5p can bind to each other in HCC exosomes and cells. It was also observed that RPL9, miR-24-3p and miR-185-5p accumulated in intracellular membrane structures. By co-culturing exosomes containing RPL9, miR-24-3p and miR-185-5p with receptor cells, it was demonstrated that the exosomes could ensure the integrity of the carried miRNAs (34) and shuttle miRNAs to recipient cells (35,36). It was suggested that RPL9 had a carrying and protective effect on miRNAs. In MHCC97H cells, an interesting phenomenon was also discovered: RPL9 could bind to miR-5100 and after downregulation of RPL9, the miR-5100 increased in cells but decreased significantly in exosomes. It was hypothesized that RPL9 mainly plays a transport role in this process; RPL9 binds to miR-5100 and translocates it into exosomes. When RPL9 expression was reduced, miR-5100 aggregated in the cells and decreased in exosomes.

RPL9, miR-24-3p and miR-185-5p are jointly involved in intercellular communication and the present study showed that RPL9 and miR-24-3p can affect the biological activity of exosomes and affect the recipient cells through exosomes to regulate tumor progression. miR-24-3p and miR-185-5p positively correlated with changes in RPL9 expression in cells. Studies have reported that miR-24-3p and miR-185-5p are enriched in patients with HCC (37,38) and can promote cancer progression (19,39). Therefore, it was hypothesized that RPL9 may be similar to other RBPs (40-42) in maintaining the stability of certain miRNAs by binding to each other and acting as a pro-oncogenic factor in an miRNA-dependent manner within cells. RPL9 was found to bind directly to miR-24-3p in cells and exosomes. Downregulation of RPL9 caused a reduction in miR-24-3p levels in exosomes and inhibited the biological activity of exosomes. Similarly, increasing miR-24-3p not only increased the content of RPL9 in exosomes but also enhanced the biological activity of exosomes and promoted the proliferation, migration and invasion of recipient cells. The present study showed that RPL9 functions as an oncogenic factor in an miRNA-dependent manner. Future

studies will focus on exploring the regulatory mechanisms of RPL9 packaging of miRNAs into exosomes (Figs. S4 and S5).

In summary, the present study showed that RPL9 has a pro-cancer effect, can carry miR-24-3p and miR-185-5p to exosomes in a mutually binding manner and modulates the biological properties of receptor HCC cells by changing the profile of exosomal miRNAs. These findings may lead to the identification of new biomarkers and development of therapeutic strategies.

Acknowledgements

Availability of data and materials

The data generated in the present study may be requested from the corresponding author.

Authors' contributions

AL and JYX conceived the study, performed most of the experiments and was a major contributor in writing the manuscript. LHL designed the study, analyzed data and revised the manuscript. WBY and WFZ collected the clinical samples and acquired data. ZHZ and SJY performed part of the experiments. DKC and JXD acquired data. PQL, JM and JXW and designed the study, analyzed data, obtained funding and supervised the study. AL and JXW confirm the authenticity of all the raw data. All authors read and approved the final manuscript.

Ethics approval and consent to participate

Tissue and serum samples were collected from patients after obtaining informed consent in accordance with a protocol approved by the Ethics Committee of Sun Yat-sen Memorial Hospital (Guangzhou, China; approval number 2023001498). All experimental procedures involving animals were performed according to the Guide for the Care and Use of Laboratory Animals (National Institutes of Health publication No. 85-23, revised 2011) and in accordance with the institutional ethical guidelines for animal experiments.

Patient consent for publication

Not applicable.

Competing interests

The authors declare that they have no competing interests.

References

1. Forner A, Reig M and Bruix J: Hepatocellular carcinoma. Lancet 391: 1301-1314, 2018.
2. Sung H, Ferlay J, Siegel RL, Laversanne M, Soerjomataram I, Jemal A and Bray F: Global cancer statistics 2020: GLOBOCAN estimates of incidence and mortality worldwide for 36 cancers in 185 countries. CA Cancer J Clin 71: 209-249, 2021.
3. van Niel G, D'Angelo G and Raposo G: Shedding light on the cell biology of extracellular vesicles. Nat Rev Mol Cell Biol 19: 213-228, 2018.
4. Kalluri R and LeBleu VS: The biology, function, and biomedical applications of exosomes. Science 367: eaau6977, 2020.
5. Pegtel DM and Gould SJ: Exosomes. Annu Rev Biochem 88: 487-514, 2019.
6. Zhang L and Yu D: Exosomes in cancer development, metastasis, and immunity. Biochim Biophys Acta Rev Cancer 1871: 455-468, 2019.
7. Tan S, Xia L, Yi P, Han Y, Tang L, Pan Q, Tian Y, Rao S, Oyang L, Liang J, *et al*: Exosomal miRNAs in tumor microenvironment. J Exp Clin Cancer Res 39: 67, 2020.
8. Corley M, Burns MC and Yeo GW: How RNA-binding proteins interact with RNA: Molecules and mechanisms. Mol Cell 78: 9-29, 2020.
9. Nussbacher JK and Yeo GW: Systematic discovery of RNA binding proteins that regulate MicroRNA levels. Mol Cell 69: 1005-1016, 2018.
10. van Kouwenhove M, Kedde M and Agami R: MicroRNA regulation by RNA-binding proteins and its implications for cancer. Nat Rev Cancer 11: 644-656, 2011.
11. Fabbiano F, Corsi J, Gurrieri E, Trevisan C, Notarangelo M and D'Agostino VG: RNA packaging into extracellular vesicles: An orchestra of RNA-binding proteins? J Extracell Vesicles 10: e12043, 2020.
12. Wei JX, Lv LH, Wan YL, Cao Y, Li GL, Lin HM, Zhou R, Shang CZ, Cao J, He H, *et al*: Vps4A functions as a tumor suppressor by regulating the secretion and uptake of exosomal microRNAs in human hepatoma cells. Hepatology 61: 1284-1294, 2015.
13. de la Cruz J, Karbstein K and Woolford JL Jr: Functions of ribosomal proteins in assembly of eukaryotic ribosomes in vivo. Annu Rev Biochem 84: 93-129, 2015.
14. Zhou X, Liao WJ, Liao JM, Liao P and Lu H: Ribosomal proteins: Functions beyond the ribosome. J Mol Cell Biol 7: 92-104, 2015.
15. Luan Y, Tang N, Yang J, Liu S, Cheng C, Wang Y, Chen C, Guo YN, Wang H, Zhao W, *et al*: Deficiency of ribosomal proteins reshapes the transcriptional and translational landscape in human cells. Nucleic Acids Res 50: 6601-6617, 2022.
16. Ebright RY, Lee S, Wittner BS, Niederhoffer KL, Nicholson BT, Bardia A, Truesdell S, Wiley DF, Wesley B, Li S, *et al*: Deregulation of ribosomal protein expression and translation promotes breast cancer metastasis. Science 367: 1468-1473, 2020.
17. Borkiewicz L, Mołoń M, Molestak E, Grela P, Horbowicz-Drożdżal P, Wawiórka L and Tchórzewski M: Functional analysis of the ribosomal uL6 protein of saccharomyces cerevisiae. Cells 8: 718, 2019.
18. National Research Council (US) Committee for the Update of the Guide for the Care and Use of Laboratory Animals: Guide for the Care and Use of Laboratory Animals. 8th edition. Washington (DC): National Academies Press (US); 2011.
19. Zhou YF, Song SS, Tian MX, Tang Z, Wang H, Fang Y, Qu WF, Jiang XF, Tao CY, Huang R, *et al*: Cystathionine β-synthase mediated PRRX2/IL-6/STAT3 inactivation suppresses Tregs infiltration and induces apoptosis to inhibit HCC carcinogenesis. J Immunother Cancer 9: e003031, 2021.
20. Liu J, Fan L, Yu H, Zhang J, He Y, Feng D, Wang F, Li X, Liu Q, Li Y, *et al*: Endoplasmic reticulum stress causes liver cancer cells to release exosomal miR-23a-3p and up-regulate programmed death ligand 1 expression in macrophages. Hepatology 70: 241-258, 2019.
21. Yang B, Feng X, Liu H, Tong R, Wu J, Li C, Yu H, Chen Y, Cheng Q, Chen J, *et al*: High-metastatic cancer cells derived exosomal miR92a-3p promotes epithelial-mesenchymal transition and metastasis of low-metastatic cancer cells by regulating PTEN/Akt pathway in hepatocellular carcinoma. Oncogene 39: 6529-6543, 2020.
22. McCullough J, Frost A and Sundquist WI: Structures, functions, and dynamics of ESCRT-III/Vps4 membrane remodeling and fission complexes. Annu Rev Cell Dev Biol 34: 85-109, 2018.
23. Pfitzner AK, Mercier V, Jiang X, Moser VFJ, Baum B, Šarić A and Roux A: An ESCRT-III polymerization sequence drives membrane deformation and fission. Cell 182: 1140-1155, 2020.
24. Gibbings DJ, Ciaudo C, Erhardt M and Voinnet O: Multivesicular bodies associate with components of miRNA effector complexes and modulate miRNA activity. Nat Cell Biol 11: 1143-1149, 2009.
25. Yao B, La LB, Chen YC, Chang LJ and Chan EK: Defining a new role of GW182 in maintaining miRNA stability. EMBO Rep 13: 1102-1108, 2012.
26. Villarroya-Beltri C, Gutiérrez-Vázquez C, Sánchez-Cabo F, Pérez-Hernández D, Vázquez J, Martin-Cofreces N, Martinez-Herrera DJ, Pascual-Montano A, Mittelbrunn M and Sánchez-Madrid F: Sumoylated hnRNPA2B1 controls the sorting of miRNAs into exosomes through binding to specific motifs. Nat Commun 4: 2980, 2013.
27. Shurtleff MJ, Yao J, Qin Y, Nottingham RM, Temoche-Diaz MM, Schekman R and Lambowitz AM: Broad role for YBX1 in defining the small noncoding RNA composition of exosomes. Proc Natl Acad Sci USA 114: E8987-E8995, 2017.
28. Hoffman DW, Davies C, Gerchman SE, Kycia JH, Porter SJ, White SW and Ramakrishnan V: Crystal structure of prokaryotic ribosomal protein L9: A bi-lobed RNA-binding protein. EMBO J 13: 205-212, 1994.
29. Warner JR and McIntosh KB: How common are extraribosomal functions of ribosomal proteins? Mol Cell 34: 3-11, 2009.
30. Huang T, Jiang C, Yang M, Xiao H, Huang X, Wu L and Yao M: Salmonella enterica serovar Typhimurium inhibits the innate immune response and promotes apoptosis in a ribosomal/TRP53-dependent manner in swine neutrophils. Vet Res 51: 105, 2020.
31. Lezzerini M, Penzo M, O'Donohue MF, Marques DSVC, Saby M, Elfrink HL, Diets IJ, Hesse AM, Couté Y, Gastou M, *et al*: Ribosomal protein gene RPL9 variants can differentially impair ribosome function and cellular metabolism. Nucleic Acids Res 48: 770-787, 2020.
32. Beyer AR, Bann DV, Rice B, Pultz IS, Kane M, Goff SP, Golovkina TV and Parent LJ: Nucleolar trafficking of the mouse mammary tumor virus gag protein induced by interaction with ribosomal protein L9. J Virol 87: 1069-1082, 2013.
33. Baik IH, Jo GH, Seo D, Ko MJ, Cho CH, Lee MG and Lee YH: Knockdown of RPL9 expression inhibits colorectal carcinoma growth via the inactivation of Id-1/NF-κB signaling axis. Int J Oncol 49: 1953-1962, 2016.
34. Kanada M, Bachmann MH, Hardy JW, Frimannson DO, Bronsart L, Wang A, Sylvester MD, Schmidt TL, Kaspar RL, Butte MJ, *et al*: Differential fates of biomolecules delivered to target cells via extracellular vesicles. Proc Natl Acad Sci USA 112: E1433-E1442, 2015.
35. Kogure T, Lin WL, Yan IK, Braconi C and Patel T: Intercellular nanovesicle-mediated microRNA transfer: A mechanism of environmental modulation of hepatocellular cancer cell growth. Hepatology 54: 1237-1248, 2011.
36. Montecalvo A, Larregina AT, Shufesky WJ, Stolz DB, Sullivan ML, Karlsson JM, Baty CJ, Gibson GA, Erdos G, Wang Z, *et al*: Mechanism of transfer of functional microRNAs between mouse dendritic cells via exosomes. Blood 119: 756-766, 2012.
37. Fan JC, Zeng F, Le YG and Xin L: LncRNA CASC2 inhibited the viability and induced the apoptosis of hepatocellular carcinoma cells through regulating miR-24-3p. J Cell Biochem 119: 6391-6397, 2018.
38. Wen Y, Han J, Chen J, Dong J, Xia Y, Liu J, Jiang Y, Dai J, Lu J, Jin G, *et al*: Plasma miRNAs as early biomarkers for detecting hepatocellular carcinoma. Int J Cancer 137: 1679-1690, 2015.
39. Zou L, Chai J, Gao Y, Guan J, Liu Q and Du JJ: Down-regulated PLAC8 promotes hepatocellular carcinoma cell proliferation by enhancing PI3K/Akt/GSK3β/Wnt/β-catenin signaling. Biomed Pharmacother 84: 139-146, 2016.
40. Bitaraf A, Razmara E, Bakhshinejad B, Yousefi H, Vatanmakanian M, Garshasbi M, Cho WC and Babashah S: The oncogenic and tumor suppressive roles of RNA-binding proteins in human cancers. J Cell Physiol 236: 6200-6224, 2021.
41. Mukohyama J, Shimono Y, Minami H, Kakeji Y and Suzuki A: Roles of microRNAs and RNA-binding proteins in the regulation of colorectal cancer stem cells. Cancers (Basel) 9: 143, 2017.
42. Vos PD, Leedman PJ, Filipovska A and Rackham O: Modulation of miRNA function by natural and synthetic RNA-binding proteins in cancer. Cell Mol Life Sci 76: 3745-3752, 2019.